JAERI-M
89-178

REFLOOD EXPERIMENTS IN SINGLE ROD CHANNEL UNDER HIGH-PRESSURE CONDITION

November 1989

Guohua XU*, Hiroshige KUMAMARU and Kanji TASAKA

日本原子力研究所
Japan Atomic Energy Research Institute

JAERI-Mレポートは，日本原子力研究所が不定期に公刊している研究報告書です。
入手の問合わせは，日本原子力研究所技術情報部情報資料課（〒319-11茨城県那珂郡東海村）あて，お申しこしください。なお，このほかに財団法人原子力弘済会資料センター（〒319-11 茨城県那珂郡東海村日本原子力研究所内）で複写による実費頒布をおこなっております。

JAERI-M reports are issued irregularly.
Inquiries about availability of the reports should be addressed to Information Division Department of Technical Information, Japan Atomic Energy Research Institute, Tokai-mura, Naka-gun, Ibaraki-ken 319-11, Japan.

編集兼発行　日本原子力研究所
印　　刷　㈱高野高速印刷

Reflood Experiments in Single Rod Channel under High-Pressure Condition

Guohua XU*, Hiroshige KUMAMARU and Kanji TASAKA

Department of Reactor Safety Research
Tokai Research Establishment
Japan Atomic Energy Research Institute
Tokai-Mura, Naka-Gun, Ibaraki-Ken

(Received October 9, 1989)

Reflood experiments were performed in the single rod test facility of Japan Atomic Energy Research Institute (JAERI). The objective of testing was to investigate thermal-hydraulic behavior during reflood. The primary parametric variables were the reflooding flow rate, initial surface temperature and linear power.

All the experiments were conducted at 1 MPa. In the experiments, saturated water was injected. The experiments covered reflooding flow rate from 0.01 to 0.18 m/s, initial surface temperature from 677 to 903 K and linear power from 0 to 2.712 kw/m. The axial power profile was uniform.

The test results show that the ratio of quench velocity to reflooding flow rate varied from 0.204 to 0.744. There are the effects of thermal parameters on the ratio of quench velocity to reflooding flow rate.

The results of high reflooding flow rate tests indicate the presence of a significant quantity of entrained liquid in the steam flow. The fluid thermocouple located at 2m from inlet of heated region was quenched at 8.5 sec after beginning of reflood and the ratio of liquid penetration velocity to quench velocity reaches 6.39, when reflooding flow rate is 0.18 m/s.

He worked in JAERI from April 1 to September 22 as a scientist of the STA Scientist Exchange Program.

* Institute of Atomic Energy (IAE), China.

The quench temperature varies between 633 K (lowest value) and 708 K (highest value). It is limitted in a narrow range, approximately in 75 K.

The experiments show the film boiling heat transfer coefficients scatter in a narrow band at the same length L_Q (length from quench front) except for the data measured at low flow rates and low linear powers.

Keywords: Reflood Experiment, Single Rod, Reflooding Flow Rate, Initial Surface Temperature, Linear Power, Quench Velocity, Liquid Penetration Velocity, Quench Temperature, Film Boiling, Heat Transfer Coefficient

高圧条件下での単一燃料棒チャンネル内の再冠水実験

日本原子力研究所東海研究所原子炉安全工学部
許　　国华*・熊丸　博滋・田坂　完二

（１９８９年１０月９日受理）

日本原子力研究所（原研）の単一燃料棒実験装置において，再冠水実験を行った。実験の目的は，再冠水時の熱水力挙動を調べることである。主要なパラメータ変数は，再冠水速度，初期表面温度及び線出力である。

全ての実験は１ＭＰａで行った。また実験では，飽和水を注入した。実験は，０.０１～０.１８ｍ／ｓの再冠水速度，６７７Ｋ～９０３Ｋの初期表面温度及び０～2.712ｋＷ／ｍの線出力をカバーしている。軸方向の出力分布は一様である。

実験では，クエンチ速度と再冠水速度の比が，０.２０４より０.７４４まで変化した。また，実験では，熱的パラメータのクエンチ速度と再冠水速度の比への効果が見られた。

高再冠水速度実験の結果は，蒸気流中にかなりの量のエントレインメント液体が存在していることを示した。再冠水速度が０.１８ｍ／ｓの時，加熱区間の入口より２ｍの位置にある流体用熱電対は，再冠水開始８.５秒後にクエンチし，液体侵透速度とクエンチ速度の比は６.３９に達した。

クエンチ温度は，６３３Ｋより７０８Ｋまで変化し，その変化は狭い範囲，約７５Ｋ以内であった。

また，実験結果は，低再冠水速度及び低線出力で得られたデータを除けば，同じL_0（クエンチフロントよりの距離）の値に対して，膜沸騰熱伝達係数は狭い範囲で変化することを示した。

１９８９年４月１日より９月２２日まで，科学技術庁原子力研究交流制度の研究員として原研で研究に従事し，とりまとめたものである。

東海研究所：〒319-11　茨城県那阿郡東海村白方字白根２－４

＊　中国原子能科学研究院

目　　次

Contents

Nomenclature

E	Emissivity
h_c	Film boiling heat transfer coefficient
h_r	Radiative heat transfer coefficient
L_c	Collapsed liquid level
L_D	Distance from quench front
H_{fg}	Latent heat of evaporation
M	Ratio of quench velocity to reflooding flow rate
P	System pressure
P_p	Linear power
q	Heat flux
s	Ratio of liquid penetration velocity to quench velocity
t	Time
t_{lp}	Liquid penetration velocity
t_q	Quench time
T_s	Saturation temperature
T_{wi}	Initial surface temperature
U_{in}	Reflooding flow rate
U_q	Quench velocity
U_{lp}	Liquid penetration velocity
Z_q	Elevation of quench front
ΔT_{sat}	Superheat of coolant
ΔT_{sub}	Inlet subcooling
ρ	Density
ε	Stefan-Boltzmann constant
λ	Thermal conductivity
μ	Dynamic viscosity

Subscripts

g	Gas phase
l	Liquid phase

1. Introduction

Single heat rod reflood heat transfer experiments were performed in the single rod test facility. The test region covered the injection condition of low pressure coolant injection system (LPCI) of pressurized water reactor (PWR) and boiling water reactor (BWR). The experiments were conducted to acquire qualitative and quantitative information regarding single rod reflood. The primary parametric variables were the reflooding flow rate, initial surface temperature and linear power. All the experiments were conducted at 1 MPa. In the experiments, the saturated water was injected, i.e. the subcooling was kept at 0 K during reflood.

The report will begin with a description of the single rod test facility and of the experimental procedures used. Then the experimental results will be discussed. Particularly, in this paper, the following topics will be discussed:

1. The effect of thermal parameters on quench front propagtion.
2. The ratio of quench velocity to reflooding flow rate.
3. Relationship between quench front and collapsed liquid level.
4. Relationship between quench front and liquid penetration.
5. Quench temperature.
6. The effect of grid spacer on reflood heat transfer.
7. Film boiling heat transfer during reflood.

2. Experimental Apparatus

A schematic diagram of the test loop is shown in Fig 1. It consists of an annular test section, pressure control system, dummy flow path, magnet valves, steam generator, hot water boiler and condenser. Water in the steam generator and hot water boiler is heated to produce high temperature, high pressure steam and water. Steam flows out from the top

1. Introduction

Single heat rod reflood heat transfer experiments were performed in the single rod test facility. The test region covered the injection condition of low pressure coolant injection system (LPCI) of pressurized water reactor (PWR) and boiling water reactor (BWR). The experiments were conducted to acquire qualitative and quantitative information regarding single rod reflood. The primary parametric variables were the reflooding flow rate, initial surface temperature and linear power. All the experiments were conducted at 1 MPa. In the experiments, the saturated water was injected, i.e. the subcooling was kept at 0 K during reflood.

The report will begin with a description of the single rod test facility and of the experimental procedures used. Then the experimental results will be discussed. Particularly, in this paper, the following topics will be discussed:

1. The effect of thermal parameters on quench front propagtion.
2. The ratio of quench velocity to reflooding flow rate.
3. Relationship between quench front and collapsed liquid level.
4. Relationship between quench front and liquid penetration.
5. Quench temperature.
6. The effect of grid spacer on reflood heat transfer.
7. Film boiling heat transfer during reflood.

2. Experimental Apparatus

A schematic diagram of the test loop is shown in Fig 1. It consists of an annular test section, pressure control system, dummy flow path, magnet valves, steam generator, hot water boiler and condenser. Water in the steam generator and hot water boiler is heated to produce high temperature, high pressure steam and water. Steam flows out from the top

of steam generator and saturated water flows out from the bottom of the hot water boiler. The steam and water flows into the dummy flow path and test section, respectively, during reflood. Finally the two-phase fluid is condensed in the condenser and the condensed water is drained.

Figure 2 shows detail of the test section. It is composed of a SUS 304 outer tube of 30 mm O.D. and 22 mm I.D. and an inner heater rod of 12.27 mm O.D. The outer tube can be divided into seven flow pieces. The inner rod is composed of three regions: non-heated entrance region of 1892 mm length, heated test region of 2000 mm length and non-heated outlet region of 317 mm length.

The sheath and the heater element are made of NCF 600 (Inconel 600) and Nichrome-5, respectively. The electric insulator inside the heater element is sintered boron nitrid (BN) and the insulator between the heater element and the sheath is packed BN.

Ten chromel-Alumel (C/A) shethed thermocouples with a sheath outer diameter of 0.5 mm are equipped in the heated region to measure the heater rod surface temperature. The thermocouple is embedded in the groove of 0.5 mm depth on the sheath outer surface. Axial locations of the thermocouples are shown in Fig. 2. The tip of the thermocouple close to the hot junction is welded to the cladding of the heated rod. The heater rod was swaged after mounting the thermocouples to ensure the tight contact of the thermocouple sheath and the heater rod cladding and to make the heat rod surface smooth.

The heated region of rod is heated indirectly by electricity with the uniform axial power distribution.

The structure of the grid spacer is shown in Fig. 2.

The pressures and temperatures of fluid are measured with pressure

transducers and thermocouples, respectively, at the inlet and outlet of the heated test region. The differential pressure across the heated test region is measured with a differential pressure transducer. The steam and water flow rates are measured upstream of the test section using orifice flow meters. Steam and water temperatures are also measured with thermocouples at the inlets of the flow meters. The pressures are measured with pressure transducers at the inlets of the flow meters.

Power supplied to the heater rod is controlled by a silicon controlled rectifier (SCR) power control system and it is measured by a wattmeter.

3. Test Conditions and Procedure

3.1 Test condition

The experimental conditions are listed in Table 1. The reflood tests were conducted in ranges of reflooding flow rate from 0.01 to 0.18 m/s, initial surface temperature from 677 to 903 K and linear power from 0 to 2.712 kw/m. The tests were preformed changing the above parameters systematically.

All the experiments were conducted under 1 MPa. The inlet subcooling is kept at OK (saturated liquid).

3.2 Test procedure

The experimental procedure is as follow:

(1) The system pressure of the facility was first set at the desired pressure.

(2) Saturated steam generated in the steam generator flowed into the test section to blow off water and to ensure the dry condition of the test section and saturated water flowed through the dummy flow path.

(3) The electric power was supplied to the heated rod.

(4) When the heated rod surface temperature reached the desired temperature, the electric power was changed to the desired value and the saturated water at desired flow rate was injected into the test section by closing magnet valve A, D and opening magnet valve B, C. The saturated steam flowed through the dummy flow path after these valve operations.

Date were recorded on a magnetic tap at the recording speed of 50 Hz or 25 Hz for each channel.

During the test, the system pressure was stabilized at the initial pressure and the supplied power was kept constant.

(5) When all the rod surface temperatures showed the cooled conditions, the power supply and the data recording were turned off, terminating the test.

4. Experimental Results

4.1 Quench front propagation and the ratio of quench velocity to reflooding flow rate

Experimental results are presented here for the effects of reflooding flow rate, initial surface temperature and linear power on quench behaviors.

Figure 3 shows the quench front propagation curves for five different reflooding flow rates, with all other conditions kept constant. It can be seen that quench front moves faster when reflooding flow rate is higher. Figure 4 shows the quench front propagation for five linear powers and Figure 5 shows the quench front propagation for four different initial surface temperatures. The test results also indicated the presence of linear power and initial surface temperature effect on quench front propagation. For the high rod power and high initial surface temperature

(3) The electric power was supplied to the heated rod.

(4) When the heated rod surface temperature reached the desired temperature, the electric power was changed to the desired value and the saturated water at desired flow rate was injected into the test section by closing magnet valve A, D and opening magnet valve B, C. The saturated steam flowed through the dummy flow path after these valve operations.

Date were recorded on a magnetic tap at the recording speed of 50 Hz or 25 Hz for each channel.

During the test, the system pressure was stabilized at the initial pressure and the supplied power was kept constant.

(5) When all the rod surface temperatures showed the cooled conditions, the power supply and the data recording were turned off, terminating the test.

4. Experimental Results

4.1 Quench front propagation and the ratio of quench velocity to reflooding flow rate

Experimental results are presented here for the effects of reflooding flow rate, initial surface temperature and linear power on quench behaviors.

Figure 3 shows the quench front propagation curves for five different reflooding flow rates, with all other conditions kept constant. It can be seen that quench front moves faster when reflooding flow rate is higher. Figure 4 shows the quench front propagation for five linear powers and Figure 5 shows the quench front propagation for four different initial surface temperatures. The test results also indicated the presence of linear power and initial surface temperature effect on quench front propagation. For the high rod power and high initial surface temperature

cases, the quench front moves slowly.

The reflooding flow rate and the quench velocity are shown in Table 2. The reflooding flow rate ranged from 0.01 m/s to 0.18 m/s and the quench velocity ranged from 0.00496 m/s to 0.0368 m/s. The ratio (M) of quench velocity to reflooding flow rate is also shown in Table 2. The ratio varied from 0.204 to 0.744. On the other hand, it is reported in Refs. [1] and [2] that the ratio of quench velocity to reflooding flow rate varied from 0.32 to 0.47. The relatively narrow range of ratio (M) in these references may be caused by narrow range of reflooding flow rate, initial surface temperature and linear power.

Figures 6 through 8 show the parametric effect on ratio (M) of quench velocity to reflooding flow rate. The effect of linear power on ratio (M) is shown in Fig. 6. The experimental results show that the ratio (M) increases with decreasing the linear power. The effect of reflooding flow rate and initial surface temperature on ratio (M) are very strong. The ratio (M) increases with decreasing the reflooding flow rate and initial surface temperature as shown in Figs. 7 and 8.

4.2 Relative position of collapsed liquid level and quench front

The relativeship between collapsed liquid level and quench front position is of interest because a collapsed liquid level greater than the quench level is suggestive of a two-phase mixture level greater than the quench level.

Figures 9 through 11 illustrate the quench and collapsed liquid levels as function of time for three tests. The quench front is observed to be well above the collapsed liquid level for the low reflooding flow rate test (RUN 612, 0.01 m/s). Other test performed at higher reflooding flow rate have some quench points above and some below the collapsed

liquid level.

4.3 Liquid penetration

A liquid penetration front is the maximum heated rod elevation where an exposed fluid thermocouple have been quenched. Figure 12 shows the quench histroy of fluid thermocouple. The liquid penetration rate is of interest because, to some extent, it characterizes the reflood.

In most of the experiments, the liquid penetration front is moving away from the quench front instead of remaining a fixed distance a head of the quench front.

Figures 13 through 15 show the effect of thermal parameters on ratio (S) of liquid penetration velocity to quench velocity. The tendency of increase in ratio S with linear power and initial surface temperature can be observed. However, the effect of linear power and initial surface temperature are rather small compared with the effect of reflooding flow rate. The effect of reflooding flow rate on ratio S is very strong. The ratio (S) increases with reflooding flow rate. The ratio (S) nearly reaches 1 when the reflooding flow rate approaches the lowest value (RUN 612, U_{in} = 0.01 m/s). This means that the liquid penetration front remains slightly in front of the quench front and fluid thermocouple quenching occurs at roughly the same time as that of the adjacent heated rod surface quenching. This may indicate low entrainment and a relatively quiescent mixture level. On the other hand, the ratio reaches 6.39 when reflooding flow rate is 0.18 m/s (RUN 652). The penetration velocity is much higher than the quench velocity. The liquid penetration front is far away from the quench front. The fluid thermocouple located at 2 m from inlet of the heated region was quenched at 8.5 sec after begining of reflood. This means large amount of water is thrown upward and the fluid

thermocouple fluid can be expected to quench much earlier than the adjacent heated rod surface. The liquid penetration velocity appears to be an indicator of entrainment. If the penetration velocity was greater than and distinct from the quench front velocity, significant entrainment was occurring. If the penetration velocity was roughly equal to the quench front velocity, significant entrainment was not occuring.

4.4 Quench temperature

Table 3 summarizes the quench temperature measured during reflood experiments. Quench temperature varies between (lowest value) 633 K and 708 K (highest value). It is limitted in the narrow range, approximately in 75 K.

In Fig. 16, the quench temperature are plotted against the initial surface temperature. The effect of initial surface temperature on quench temperature is not observed. Figures 17 and 18 show the effect of reflooding flow rate and linear power on quench temperature, respectively. It can be seen that the quench temperature was weekly dependent on linear power. The test results show the quench temperature increases with decreasing the reflooding flow rate when the reflooding flow rate is lower than 0.1 m/s. The quench temperature is nearly the same for reflooding flow rates of 0.1 m/s and 0.18 m/s.

Some investigator discovered the effect of grid spacer on quench temperature. In this experiment, the effect of grid spacer on quench temperature is not seen.

In Fig. 19, the quench temperature are plotted against pressures together with other investigator's data. Hein et al[6] measured the minimun film boiling temperature with a internally flooded pipe for a pressure range of 0.5 to 21 MPa. Koizumi, et al.[7] measured the quench

temperature at Two-phase Flow Test Facility (TPTF). The test section is composed of 25 (5x5) indirected electric heater rods. The test condition ranged 0.5-12 MPa for pressure, 0.3-1.2 m/s for inlet reflooding flow rate and 0 K for inlet subcooling (Saturated liquid). The experimental data are shown in Fig. 19. The present data are very close to these data with tube and rod bundles.

In Fig. 19, some other correlaiton and test data[2][8]-[11] are shown for comparison. The saturation temperature are also shown for comparison.

4.5 Effect of grid spacer on reflood

Some experimental works[3][4][5] under low pressur have been conducted in order to investigate the effect of grid spacer on reflood heat transfer. The effect of grid spacer on reflood heat transfer have been clarified in these works.

The results of reflood tests performed at the single rod test facility indicated the presence of grid spacer effect on the surface temperature profiles and quench time in some tests. Examples of the temperature profiles are presented in Fig. 20. There is a noticeable lowering of the rod temperature at 1.58 m of elevation. This corresponds to the location of downstream of the grid spacer.

The other grid spacers are installed at 0.685 m and 1.133 m of elevation. Because there are no thermocouples near these grid spacers, the effect of these grid spacers on temperature profiles did not appear.

Quenching behavior is also affected by the grid spacer. Figure 3 through 5 show the effect of grid spacer on quench time downsteam of the grid spacer. Quench occurs earlier here in some experiments.

The effect of grid spacer on quench time and rod surface temperature depends on thermal parameters. As shown in Fig. 4, the effect of grid

spacer increases with decresing the linear power. Significant effect was not observed when the linear power is less than 1.416 kw/m (the initial surface temperature is 860 K and reflooding flow rate is 0.025 m/s). Figure 3 shows the effect of reflooding flow rate on quench front propagation. The effect of grid spacer increases with reflooding flow rate. No significant effect was observed when the reflood flow rate is less than 0.025 m/s. The effect of initial surface temperature on quench front propagation is shown in Fig. 5. The effect of grid spacer increases with decreasing the initial surface temperature. When initial surface temperature exceeds 860 K, no significant effect appears.

4.6 Film boiling heat transfer coefficient

Figure 21 shows the typical heater rod surface temperature transient measured in the experiment. From this rod surface temperature transient, rod surface heat fluxes were calculated by a heat conduction calculation package of the RELAP5/MOD2. The integral form of the heat conduction equation is

$$\iiint_V (T,\bar{x}) \frac{\partial T}{\partial t} (\bar{x},t)dv = \iint_S K(T,\bar{x})\Delta T(\bar{x},t)ds + \iiint S(\bar{x},t)dv \quad \cdots(1)$$

where K : thermal conductivity,

s : surface,

S : internal heat source,

t : time,

T : temperature,

$\bar{x}$: space coordinates

ρ : volumetric heat capacity

In the calculation of heat fluxes q, the axial heat conduction was

not taken into consideration. Reference [12] indicated the axial heat conduction along the rod can be neglected even at the stage just before the quench time. The effect of axial heat conduction is limited to a short length (about 2 cm) of rod at quench front during the reflood phase.

The boundary condition is the measured rod surace temperature.

The following equations were used for the calculation of film boiling heat transfer coefficient h_c :

$$h_t = h_c + h_r = \frac{q}{T_w - T_s} \quad \cdots\cdots (2)$$

$$h_r = E\epsilon(T_w^4 - T_{sat}^4) \; / \; \Delta T_{sat} \quad \cdots\cdots (3)$$

The emissivity of the heater rod surface (Inconel 600) is assumed to be 0.65[13][14].

Figures 22 through 25 show the test results of film boiling heat transfer coefficient. In the figures representative length L_Q is the distance from the quench front. Figure 22 indicates that except for RUN 612, h_c are scattered in a narrow band at the same length. The reflooding flow rate is much lower for RUN 612 (U_{in} = 0.01 m/s). Figures 23 through 25 show that h_c are scattered in the same narrow band for different initial surface temperatures, linear powers and elevations except for RUN 522 and 512 (P_p = 0.78 kw/m and 0 kw/m). The film boiling heat transfer coefficient for low linear powers is much lower than that for high linear powers.

To predict the film boiling heat trasnfer during reflood phase, many investigations have been conducted.

Bromley[15] developed the theory for vertical heated surface as well as for a horizontal heated cylinder, and it is expressed as

$$h_c = C\left[\frac{\lambda_g^3 \rho_g(\rho_l - \rho_g)H_{fg}'}{L\,\mu_g \Delta T_{sat}}\right]^{1/4} \quad \cdots\cdots (4)$$

where the constant C lies between 0.667 and 0.943.

An empirical reflood heat transfer correlation[16] was developed by using the PWR-FLECHT data base on upward flooding experiments. For the quasi-steady period, the following correlation was derived:

$$h_c = 261.2\,\{1-\exp(-9.84\,U_{in})\}\{0.714 + 0286\,[1-\exp(-0.16843\,P/\,U_{in}^2)]\} + 215.9\exp(-5.9\,U_{in})\exp(-3.937L_Q) \quad \cdots\cdots (5)$$

Sudo[17] developed an empirical correlation for the heat transfer coefficient of the saturated and subcooled film boilig regimes under simulated reflood condition. The correlation is

$$h_c = h_{sat}\,(1 + 0.0025\,\Delta T_{sub}) + 3/4^{hr} \quad \cdots\cdots (6)$$

where $h_{sat} = 0.94\,[\lambda_g^3 \rho_g(\rho_l-\rho_g)H_{fg}'\,/\,L_Q \mu_g \Delta T_{sat}]^{1/4}$

$h_r = E\varepsilon(T_w^4 - T_{sat}^4)\,/\,\Delta T_{sat}$

$H_{fg}' = H_{fg}\,[1 + 0.4C_p\Delta T_{sat}\,/\,H_{fg}]^2$

The correlation for saturated film boiling is similar to Ellion's correlation except for factor 0.94 and the use of H_{fg}'.

The experimental data are compared with these correlations in Figs. 26 and 27. In the Figures, beside Sudo's correlation and yeh's correlation, Modified Bromley correlation is used for comparison (factor : 0.62).

Modified Bromley correlation and yeh's correlation underestimate the heat transfer coefficient over the region of the present experimental conditions except for low reflooding flow rate and low linear power.

Sudo's correlation predicts the experimental results of single rod

experiments well for the representative length L_Q from 2.5 to 40 cm. However, it's predictions are higher than results at the low reflooding flow rate and low liner power. In the experiments, quality at quench front ranges from 0 to 0.324.

Figure 28 shows the comparison of calculated heat transfer coefficients (using sudo's correlation) with experimental data (except for RUN 612, 522, 512). The agreement between the calculation and the data is approximately within a range of ± 25%.

5. Conclusions

Reflood experiments were performed in an annular flow channel with an uniformly heated rod under test conditions of the reflooding flow rate from 0.01 to 0.18 m/s, initial surface temperature from 677 to 903 K and linear power from 0 to 2.712 kw/m. From the experimental results and discussions, it is concluded as follows:

(1) In reflood tests, the ratio of quench velocity to reflood flow rate varied from 0.204 to 0.744. The ratio depends on thermal parameters, i.e the reflooding flow rate, initial surface temperature and linear power.

(2) The effect of reflooding flow rate, initial surface temperature and linear power on the ratio (S) of liquid penetration velocity to quench velocity was clarified. The ratio (S) reaches nearly 1 when reflood flow rate becomes low. In a high reflood flow rate, the penetration front is far away from quench front. This indicates the existence of significant liquid entrainment in a high reflood flow rate.

(3) Quench temperatures varied between 633 K (lowest) and 708 K

experiments well for the representative length L_Q from 2.5 to 40 cm. However, it's predictions are higher than results at the low reflooding flow rate and low liner power. In the experiments, quality at quench front ranges from 0 to 0.324.

Figure 28 shows the comparison of calculated heat transfer coefficients (using sudo's correlation) with experimental data (except for RUN 612, 522, 512). The agreement between the calculation and the data is approximately within a range of ± 25%.

5. Conclusions

Reflood experiments were performed in an annular flow channel with an uniformly heated rod under test conditions of the reflooding flow rate from 0.01 to 0.18 m/s, initial surface temperature from 677 to 903 K and linear power from 0 to 2.712 kw/m. From the experimental results and discussions, it is concluded as follows:

(1) In reflood tests, the ratio of quench velocity to reflood flow rate varied from 0.204 to 0.744. The ratio depends on thermal parameters, i.e the reflooding flow rate, initial surface temperature and linear power.

(2) The effect of reflooding flow rate, initial surface temperature and linear power on the ratio (S) of liquid penetration velocity to quench velocity was clarified. The ratio (S) reaches nearly 1 when reflood flow rate becomes low. In a high reflood flow rate, the penetration front is far away from quench front. This indicates the existence of significant liquid entrainment in a high reflood flow rate.

(3) Quench temperatures varied between 633 K (lowest) and 708 K

(highest). It is limited in a narrow range, approximately in 75 K.

(4) The results of reflood tests performed in this facility indicated the presence of grid spacer effect on surface temperature profiles and quench times. There was a noticeable the rod temperature and an earlier occurrence of quench downstream of the grid spacer in some tests.

(5) The film boiling heat transfer coefficients scatter in a narrow band at the same length L_Q. Sudo's correlation predicts the experimental results well for the representative length L_Q from 2.5 to 40 cm and quality at quench front from 0 to 0.324 except for the data measured at low flow rates and low linear powers.

Acknowledgments

The authors wish to express their sincere thanks to Mr. H. Murata of the Japan Atomic Energy Research Institute and Mr. H. Yamada and other members of Nuclear Engineering Co. to conduct the experiments. They are also indebted Mr. E. Umeki of ISL Co. for data processing, Mr. Y. Mimura of ISL Co. for assisting RELAP5 calculation and Miss M. Kikuchi of Nihon Computer Bureau for typing the manuscript.

(highest). It is limited in a narrow range, approximately in 75 K.

(4) The results of reflood tests performed in this facility indicated the presence of grid spacer effect on surface temperature profiles and quench times. There was a noticeable the rod temperature and an earlier occurrence of quench downstream of the grid spacer in some tests.

(5) The film boiling heat transfer coefficients scatter in a narrow band at the same length L_Q. Sudo's correlation predicts the experimental results well for the representative length L_Q from 2.5 to 40 cm and quality at quench front from 0 to 0.324 except for the data measured at low flow rates and low linear powers.

Acknowledgments

The authors wish to express their sincere thanks to Mr. H. Murata of the Japan Atomic Energy Research Institute and Mr. H. Yamada and other members of Nuclear Engineering Co. to conduct the experiments. They are also indebted Mr. E. Umeki of ISL Co. for data processing, Mr. Y. Mimura of ISL Co. for assisting RELAP5 calculation and Miss M. Kikuchi of Nihon Computer Bureau for typing the manuscript.

References

(1) Hyman,C. R., et al.: NUREG/CR-2455

(2) Anklam, T. M.,: NUREG/CR-2144 ORNL/NUREG/TM-446

(3) SUGIMOTO, T., et al.: J. Nucl. Sci. Technol, 21[2] 103-114 (1984)

(4) Veteau, J. M., et al.: NUREG/CP-0048, Vol.1, 402-427

(5) Ihle, P., et al.: NUREG/CP-0043 417-444

(6) Hein, D., et al.: NUREG/CP-0064 (1984)

(7) Koizumi, Y., et al.: to be published in Nucl. Eng. Des.

(8) Cheng, S. C., et al.: Int. J. Heat Mass Transfer., 28[1] 235-243 (1985)

(9) Berlin, I. I., et al.: Inzh. Fiz. Zh., 24[2] 139-143 (1973)

(10) Groeneveld, D. C. et al.: Proc. 7th. Int. Heat Transfer Conf., Munchen, Vol. 4. FB37 393-398 (1982)

(11) Lienhard, J. H.: Chen. Eng. Sci., 31[9] 847-849 (1976)

(12) OSAKABE, M.: J. Nucl. Sci. Technol., 20[7] 559-570 (1983)

(13) MURAO, Y.: J. Nucl. Sci. Technol., 18[4] 275-284 (1981)

(14) Touloukain, Y. S., et al.: "Thermophysical properties of Matter," Vol 7, P_{972} (1970)

(15) Bromley, L. A., et al.: Chem. Eng. Progr., 46, 221 (1950)

(16) Yeh, H. C., et al.: Nucl. Technol., 46[MID-DEC. 1979], (1979)

(17) SUDO, Y.: J. Nucl. Sci. Technol., 17[7] 516-530 (1980)

Table 1 Experimental conditions

RUN	P(MPa)	U_{in}(m/s)	P_p(kw/m)	ΔT_{sub}(K)
512	1	0.025	0	0
522	1	0.025	0.78	0
542	1	0.025	2.064	0
552	1	0.025	2.712	0
612	1	0.01	1.416	0
622	1	0.025	1.416	0
623	1	0.025	1.416	0
633	1	0.05	1.416	0
642	1	0.10	1.416	0
652	1	0.18	1.416	0
712	1	0.025	1.416	0
722	1	0.025	1.416	0
732	1	0.025	1.416	0

Table 2 Ratio of quench velocity to reflooding flow rate

RUN	U_{in}(m/s)	U_q(m/s)	U_q/U_{in}
512	0.025	0.0134	0.536
522	0.025	0.0133	0.532
542	0.025	0.0115	0.460
552	0.025	0.0112	0.448
612	0.01	0.00496	0.496
622	0.025	0.0117	0.468
623	0.025	0.0120	0.480
633	0.05	0.0212	0.424
642	0.10	0.0298	0.298
652	0.18	0.0368	0.204
712	0.025	0.0186	0.744
722	0.025	0.0161	0.644
732	0.025	0.0133	0.532

Table 3 Quench temperature and quench time

test	Z(m)	T_{wi}(K)	T_q(K)	t_q(s)
RUN 512	1.00	853	665	80
RUN 512	1.42	863	659	107
RUN 512	1.58	833	640	114
RUN 512	1.82	853	633	134
RUN 522	1.00	883	658	81
RUN 522	1.42	893	667	108
RUN 522	1.58	865	645	117
RUN 522	1.82	878	645	137
RUN 542	1.00	883	663	99
RUN 542	1.42	893	668	130
RUN 542	1.58	868	648	135
RUN 542	1.82	883	663	158
RUN 552	1.00	878	668	104
RUN 552	1.42	888	666	140
RUN 552	1.58	863	661	136
RUN 552	1.82	853	673	162
RUN 612	1.00	878	668	192
RUN 612	1.42	898	668	290
RUN 612	1.58	851	708	325
RUN 612	1.82	808	693	367
RUN 622	1.00	863	653	90
RUN 622	1.42	873	668	119

Table 3 (continued)

RUN 623	1.58	843	638	132
RUN 622	1.82	863	648	155
RUN 623	1.00	893	653	93
RUN 623	1.42	903	653	123
RUN 623	1.58	878	648	131
RUN 623	1.82	893	653	152
RUN 633	1.00	868	643	64
RUN 633	1.42	878	653	75
RUN 633	1.58	858	648	65
RUN 633	1.82	883	653	86
RUN 642	1.00	833	631	52
RUN 642	1.42	845	633	57
RUN 642	1.58	823	641	46
RUN 642	1.82	868	633	61
RUN 652	1.00	833	635	44.5
RUN 652	1.42	848	633	49.5
RUN 652	1.58	819	653	33.5
RUN 652	1.82	873	643	49.5
RUN 712	1.00	713	646	63
RUN 712	1.42	703	643	83
RUN 712	1.58	677	637	80
RUN 712	1.82	679	647	98
RUN 722	1.00	757	659	73
RUN 722	1.42	773	648	96

Table 3 (continued)

RUN 722	1.58	737	648	94
RUN 722	1.82	737	648	113
RUN 732	1.00	838	653	82
RUN 732	1.42	843	658	111
RUN 732	1.58	818	646	113
RUN 732	1.82	813	651	137

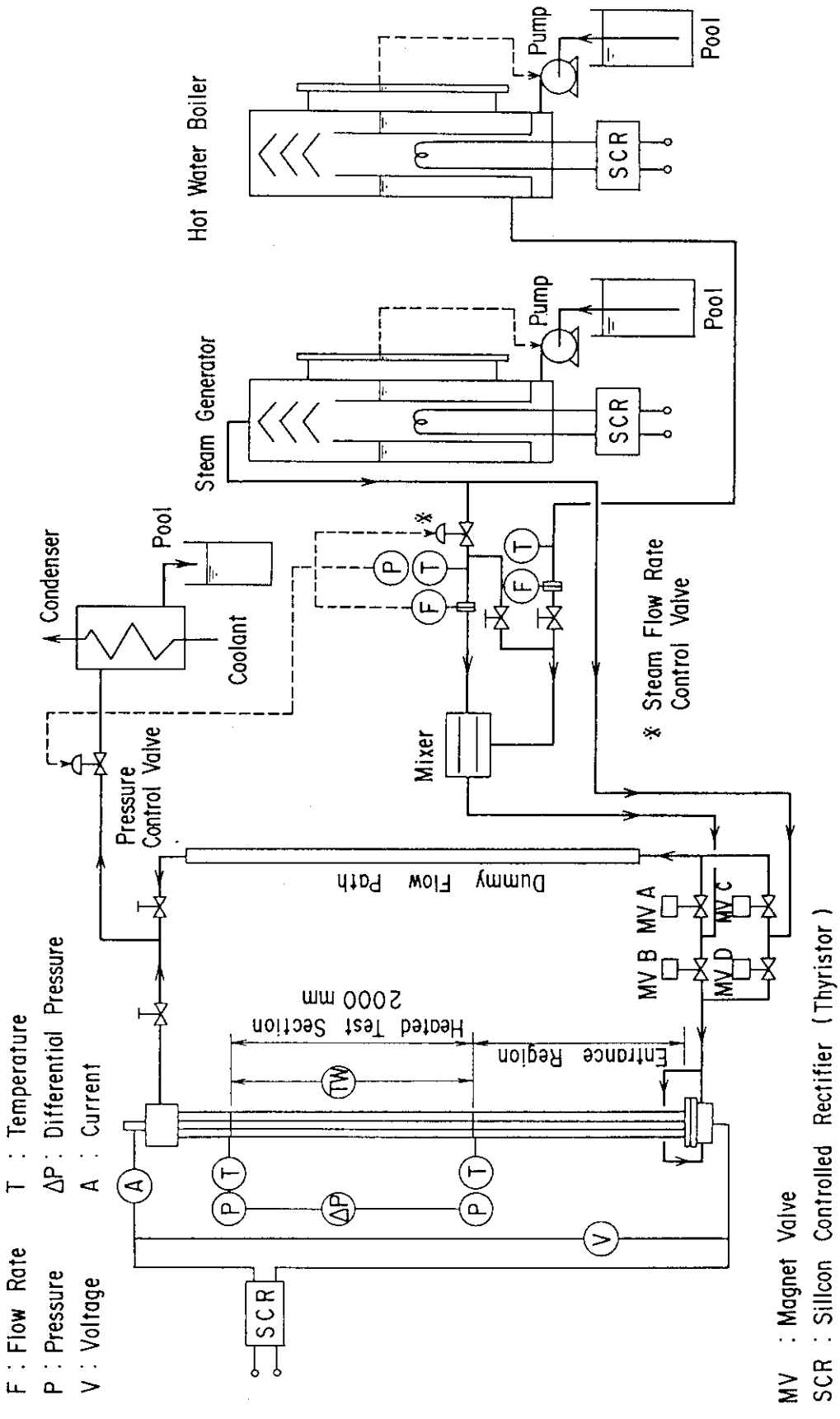

Fig. 1 Flow diagram of single rod test facility

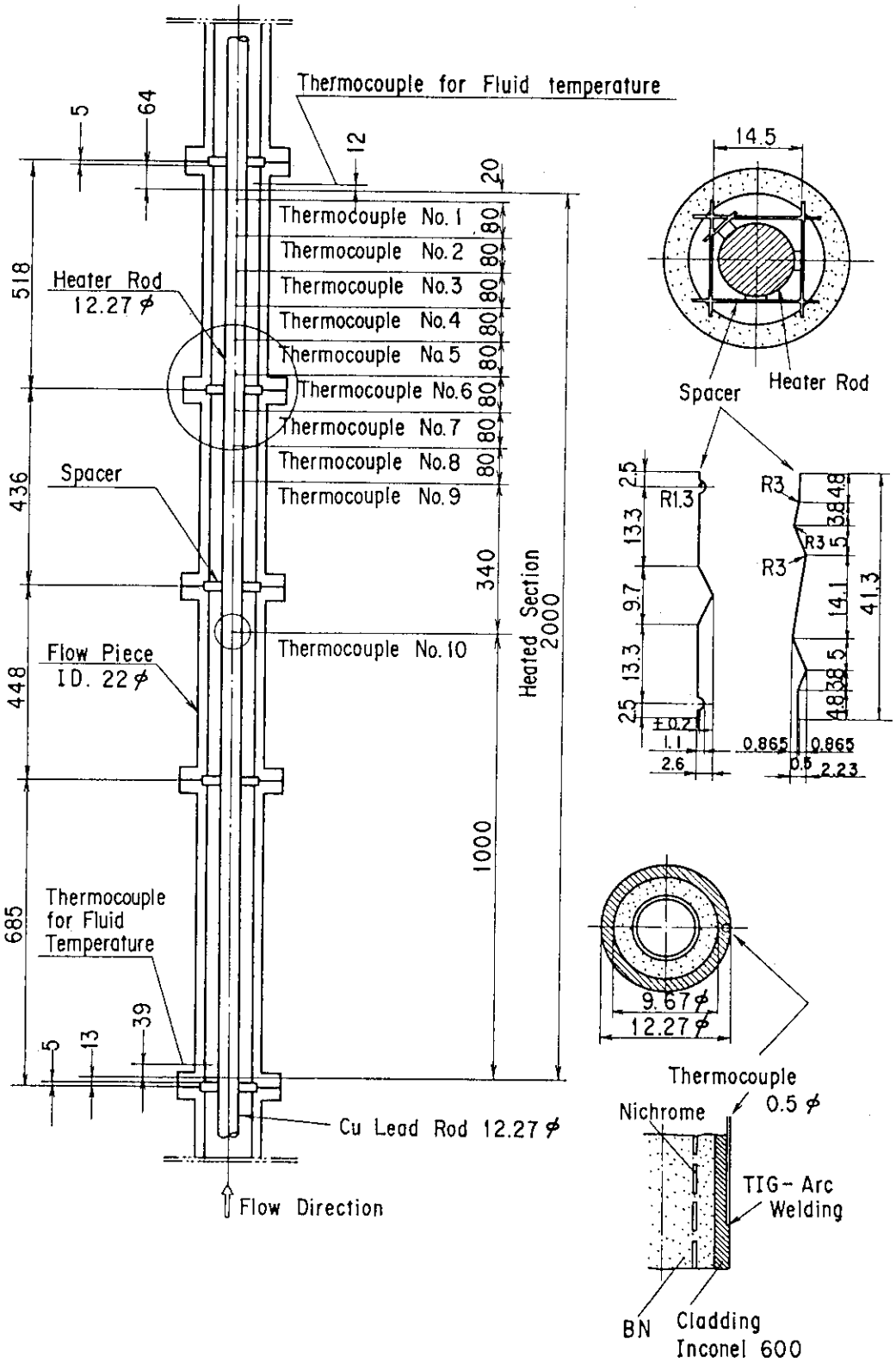

Fig. 2 Heater rod used in present experiment

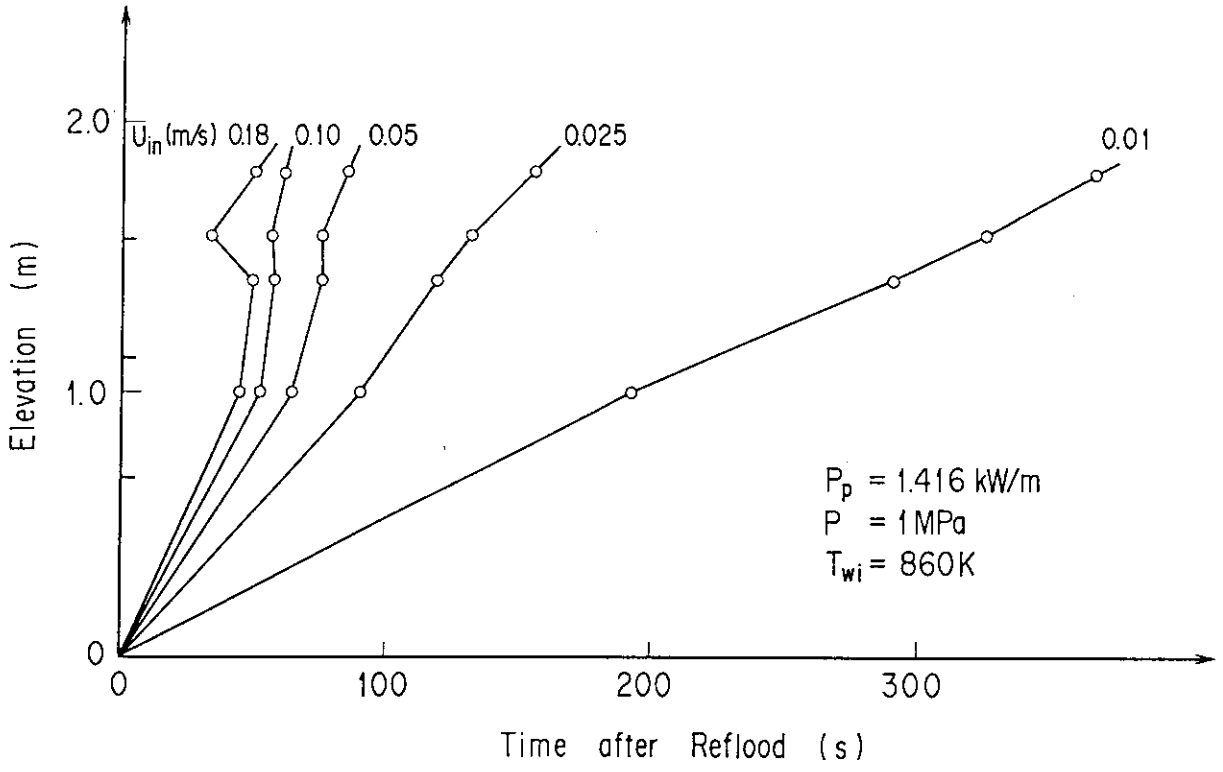

Fig. 3 Quench front propagation

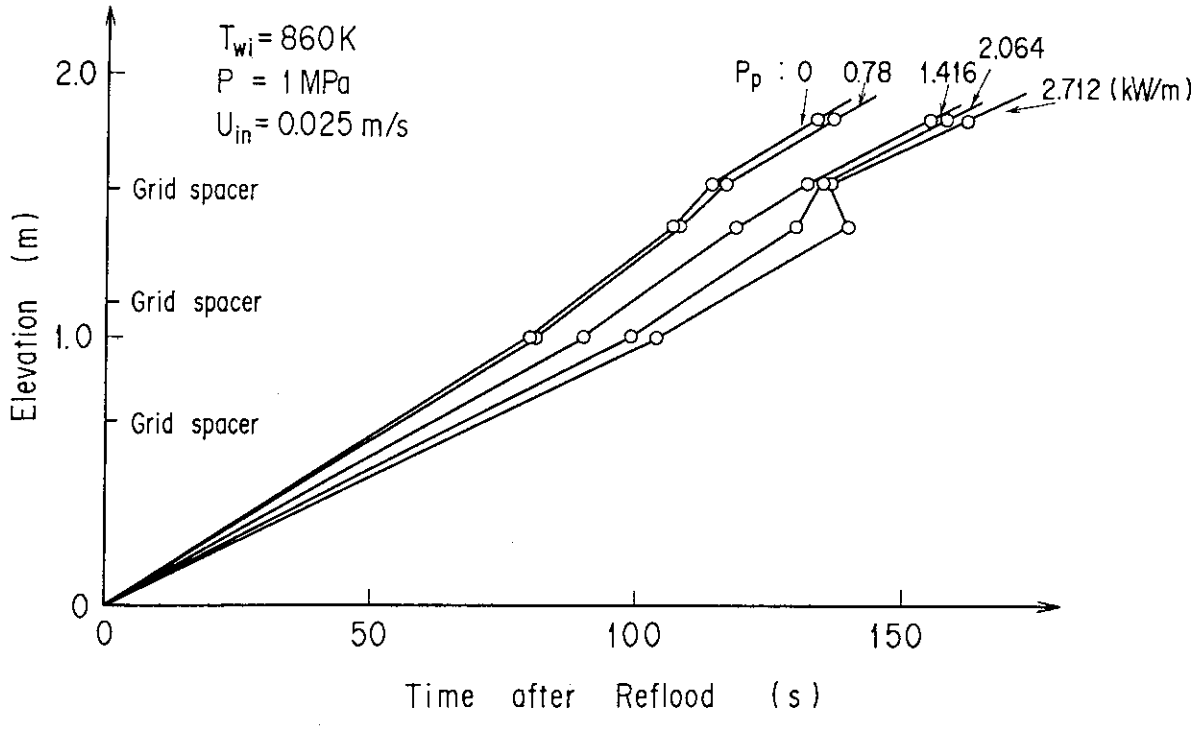

Fig. 4 Quench front propagation

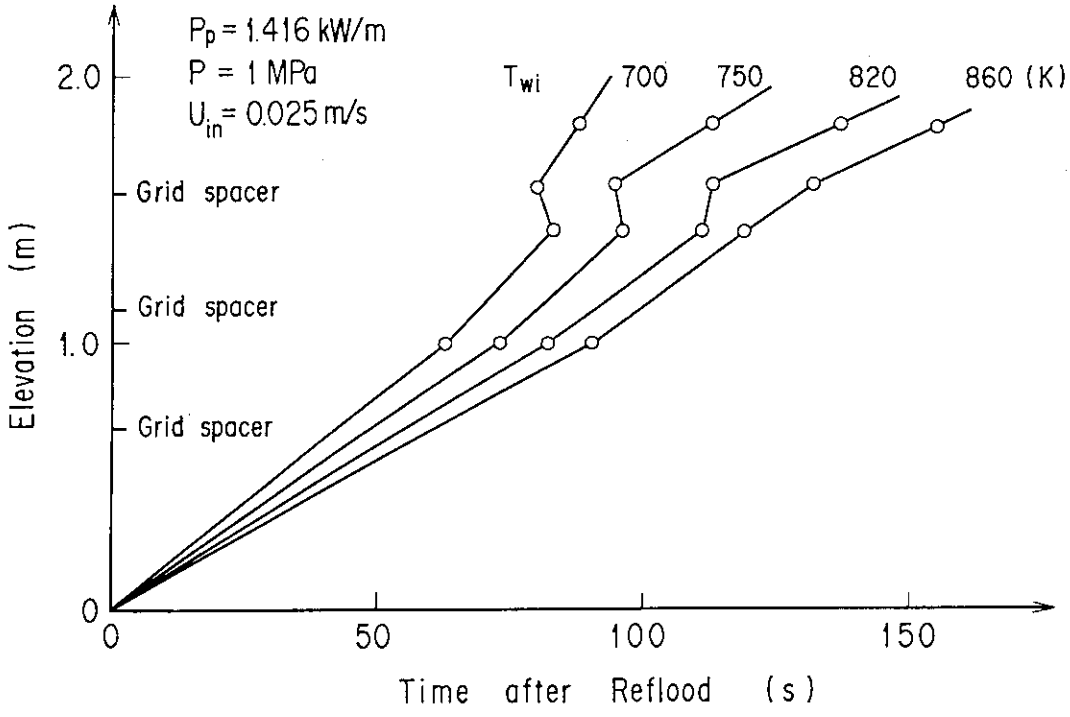

Fig. 5 Quench front propagation

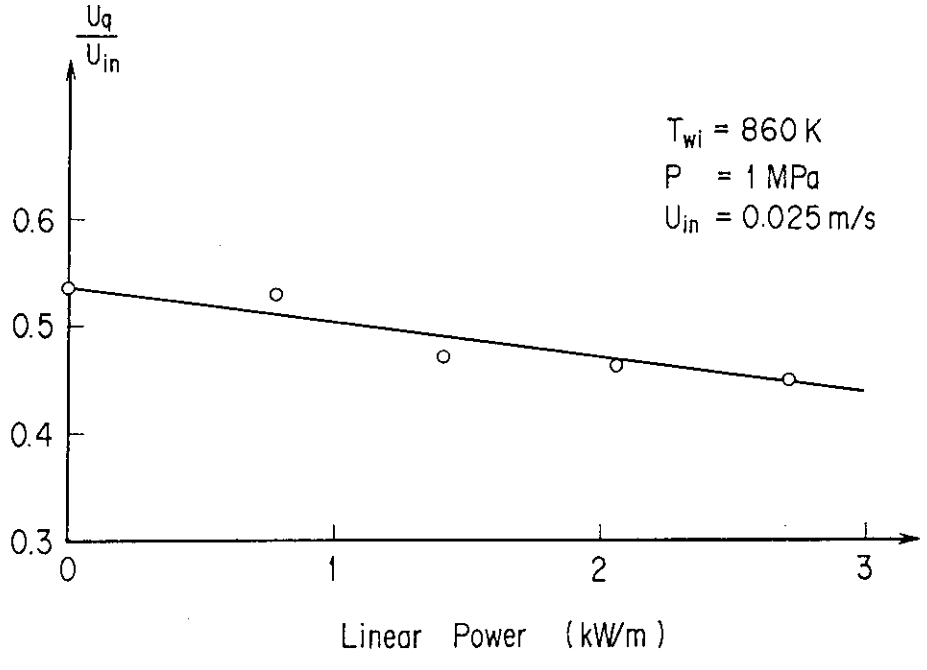

Fig. 6 The ratio of quench velocity to reflooding flow rate

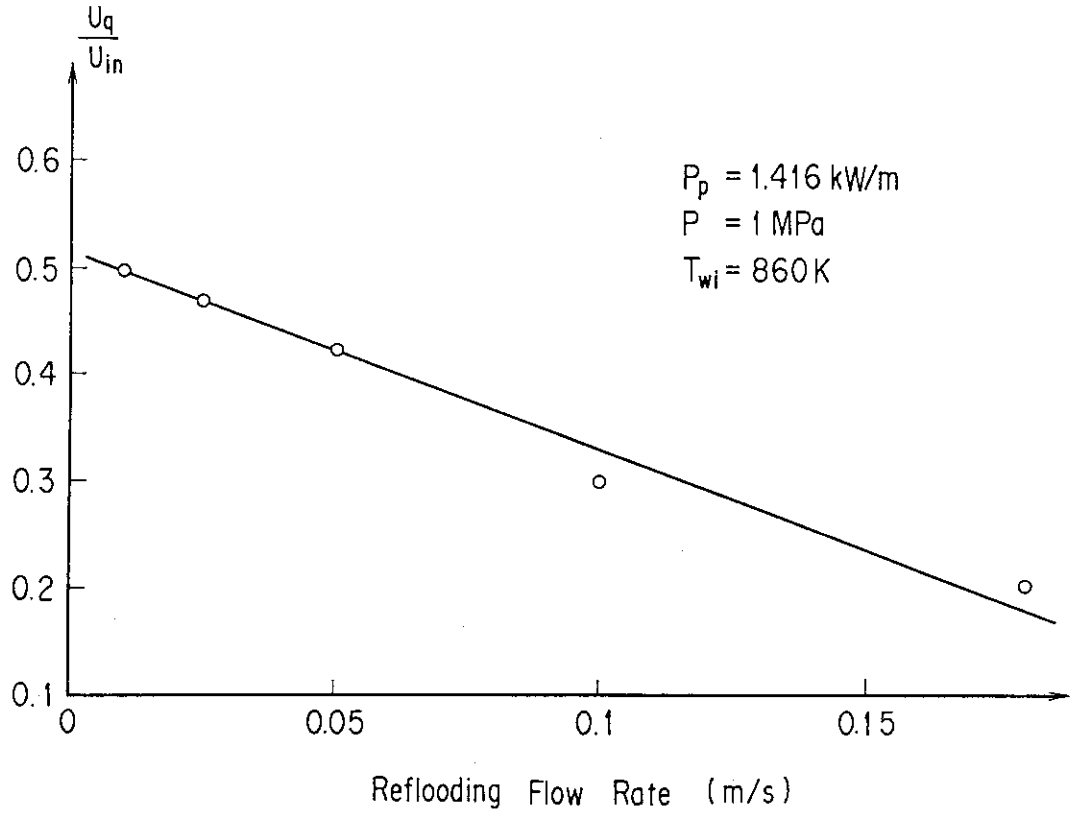

Fig. 7 The ratio of quench velocity to reflooding flow rate

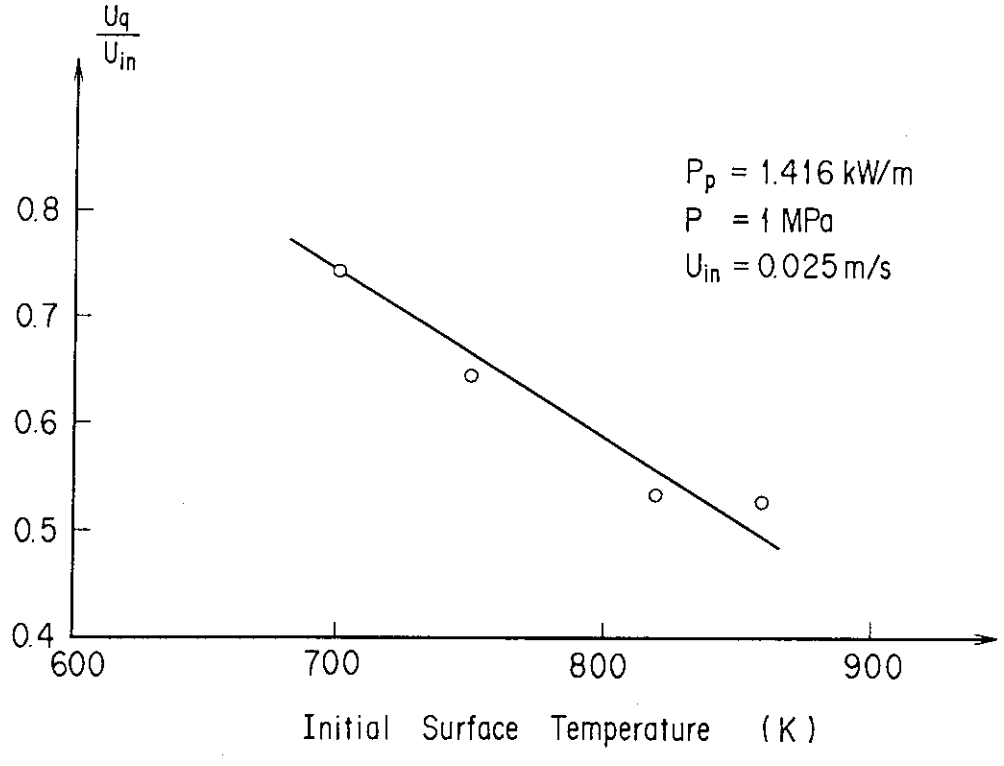

Fig. 8 The ratio of quench velocity to reflooding flow rate

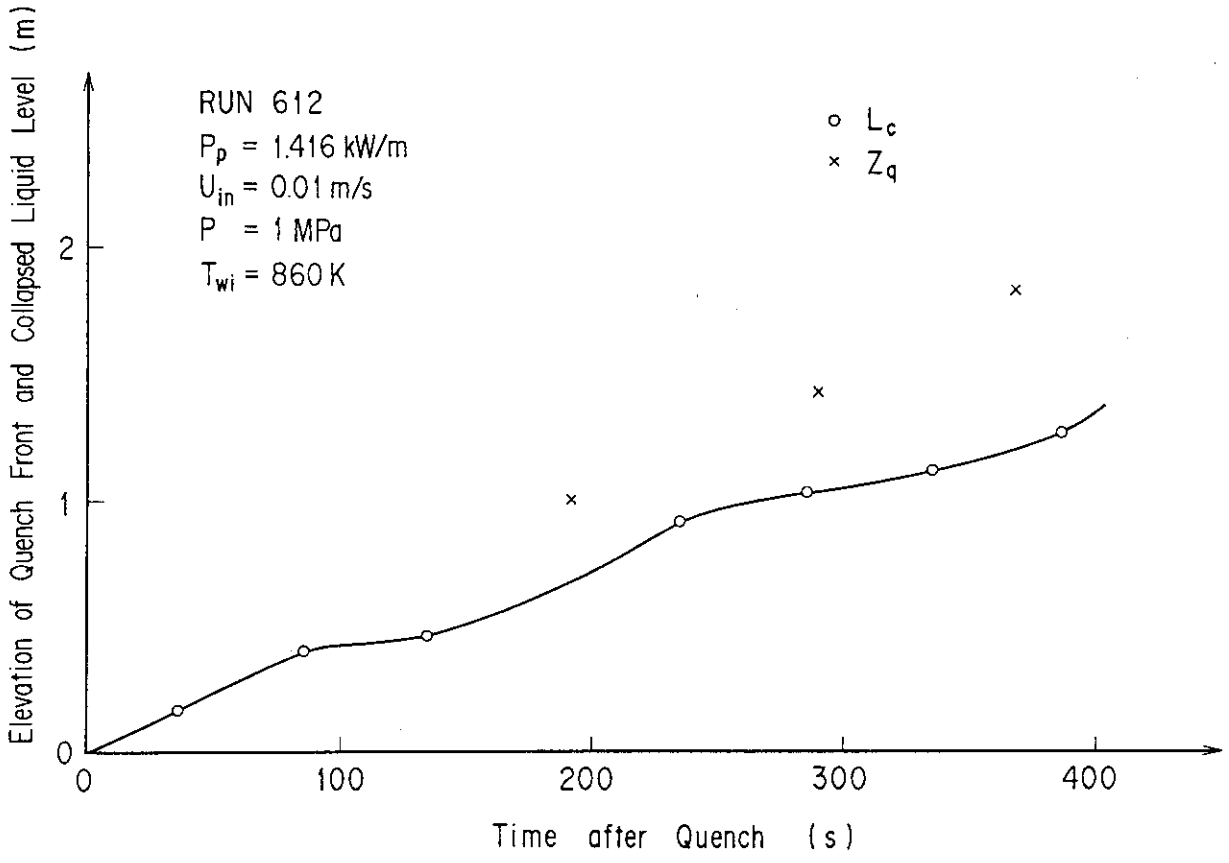

Fig. 9 Quench front and collapsed liquid level vs time

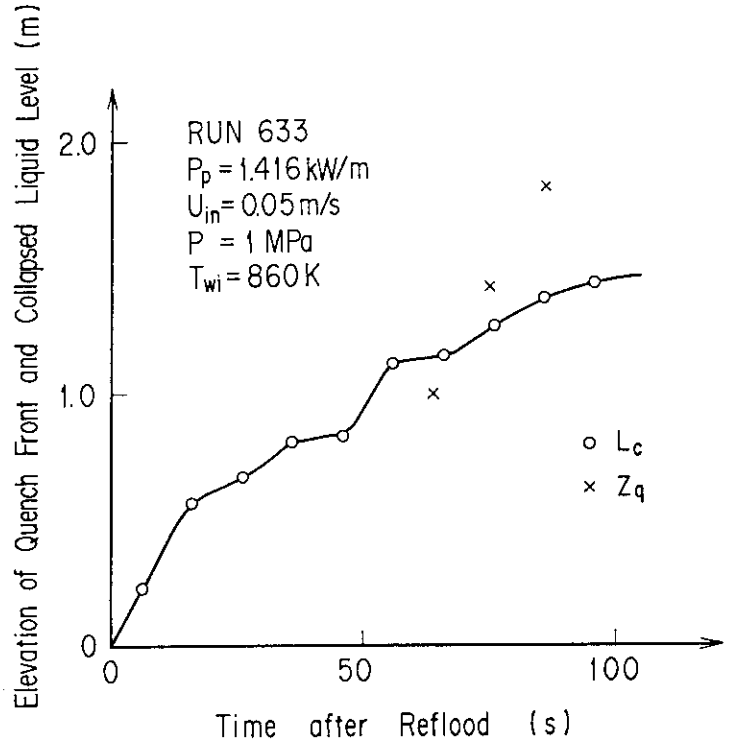

Fig. 10 Quench front and collapsed liquid level vs time

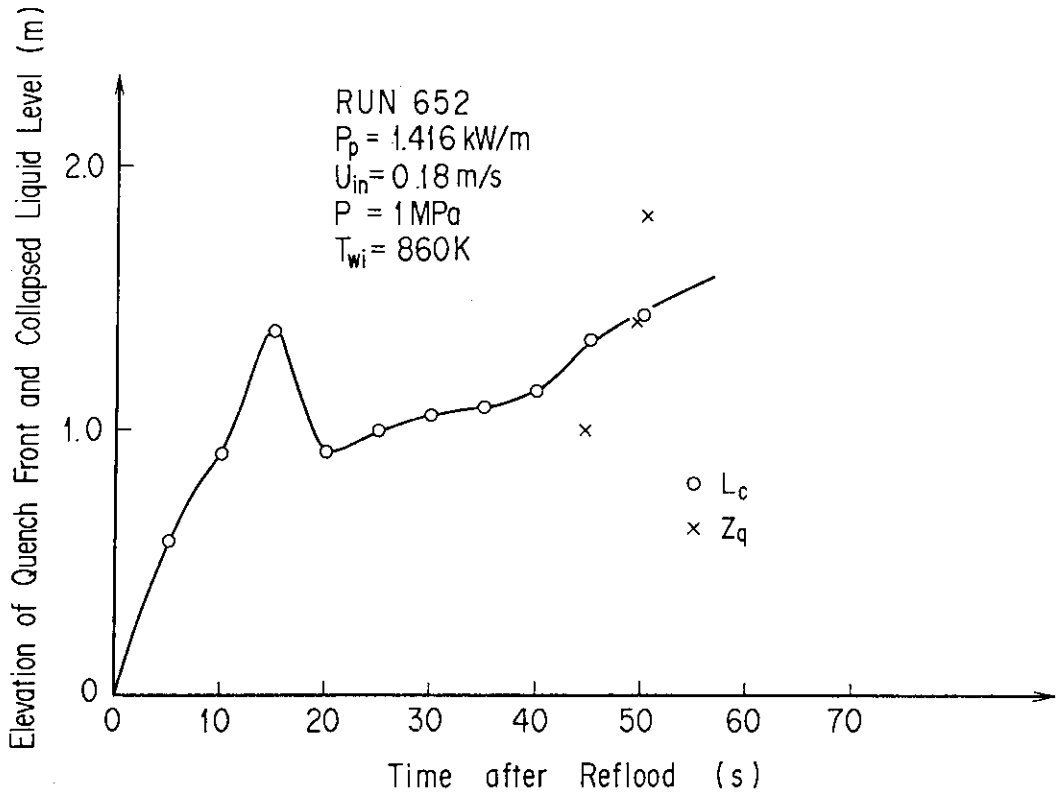

Fig. 11 Quench front and collapsed liquid level vs time

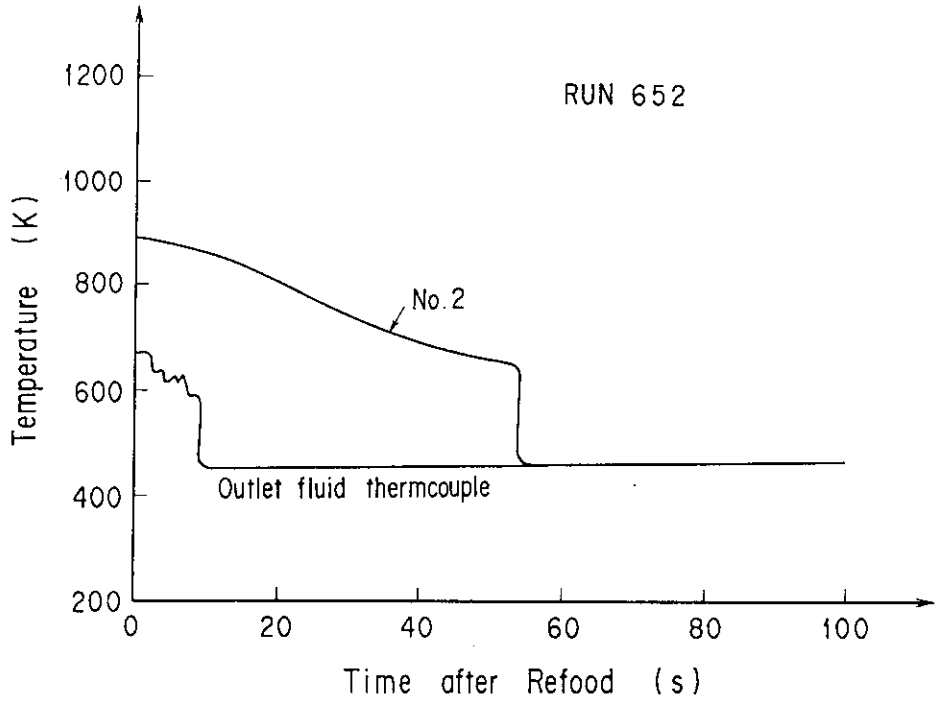

Fig. 12 Quench history of fluid thermocouple

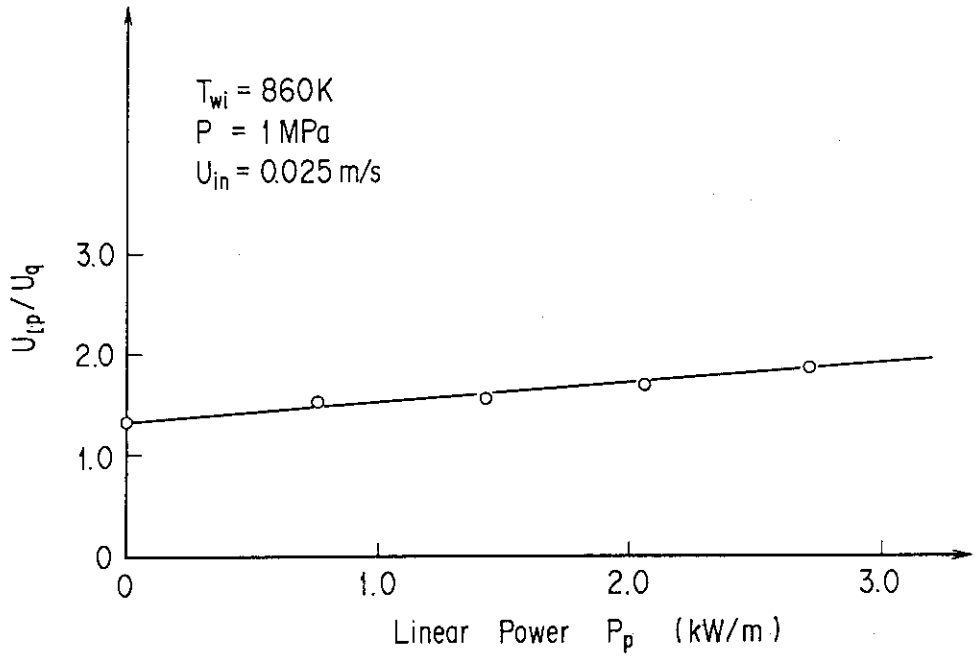

Fig. 13 Ratio of average liquid penetration velocity to average quench velocity

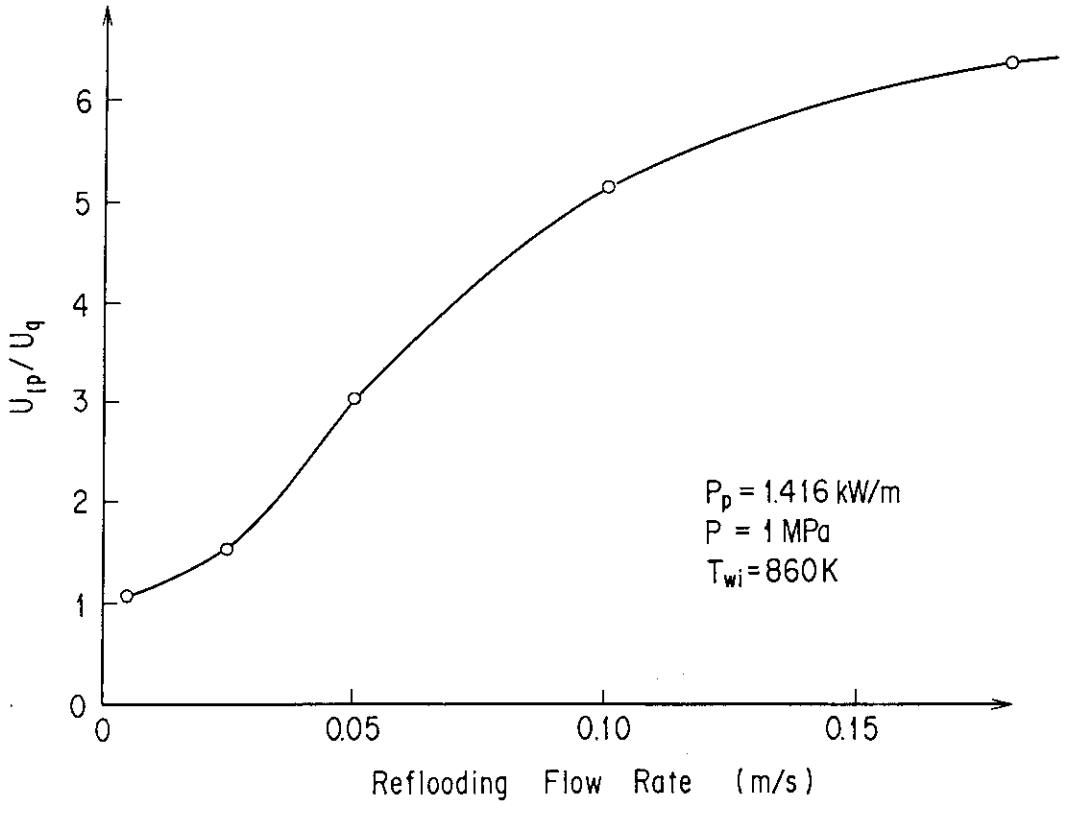

Fig. 14 Ratio of average liquid penetration velocity to avarage quench velocity

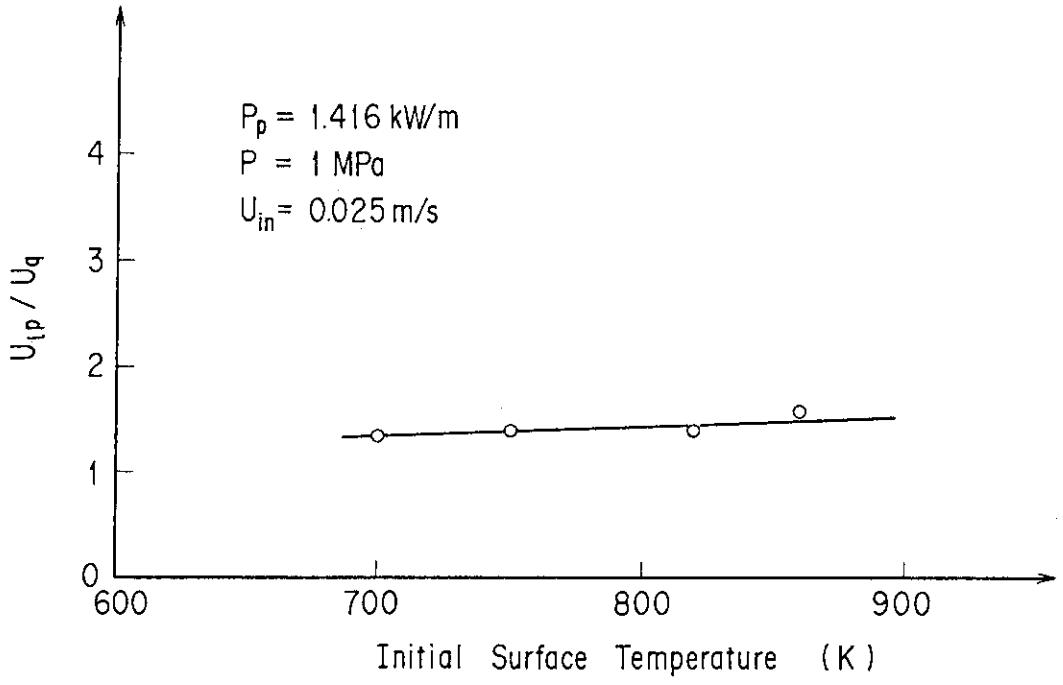

Fig. 15 Ratio of average liquid penetartion velocity to average quench velocity

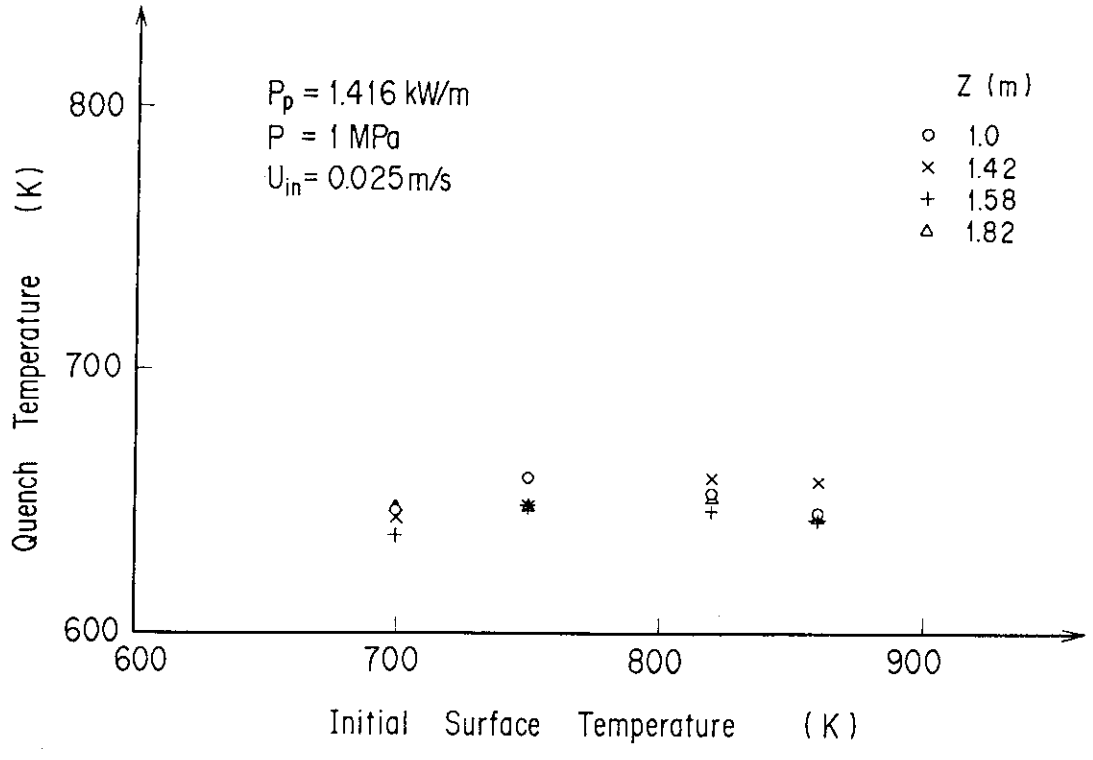

Fig. 16 Effect of initial temperature on quench temperature

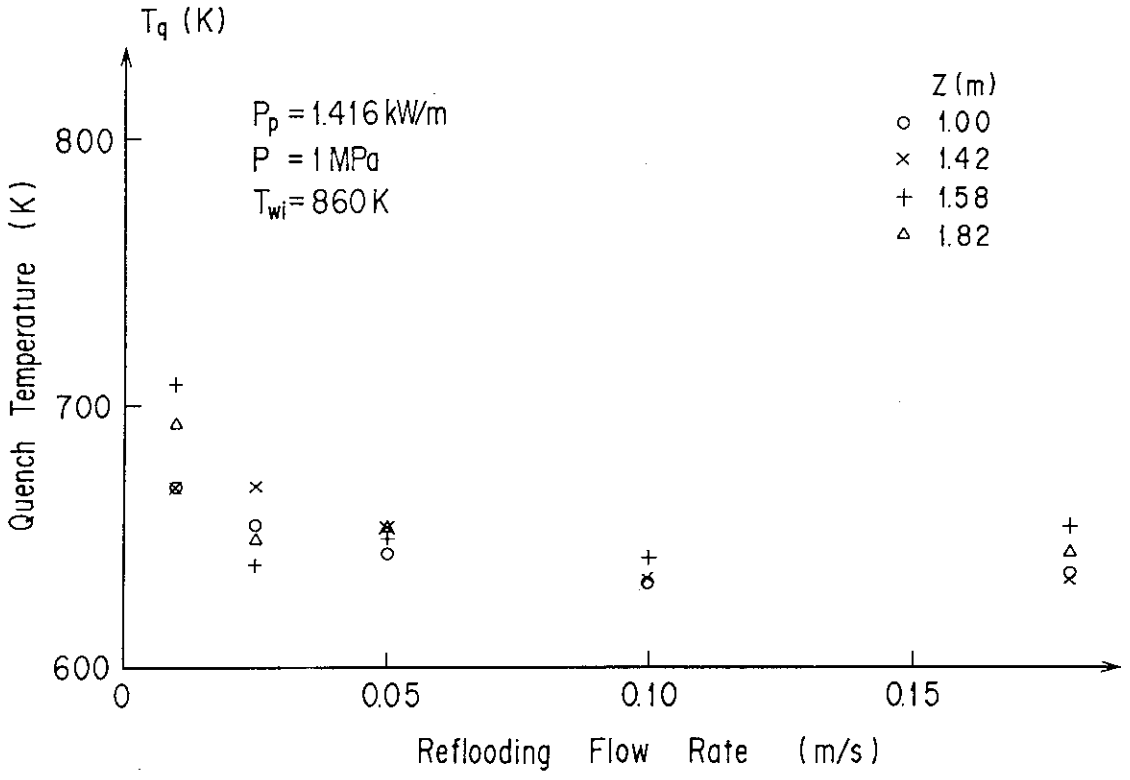

Fig. 17 Effect of reflooding flow rate on quench temperature

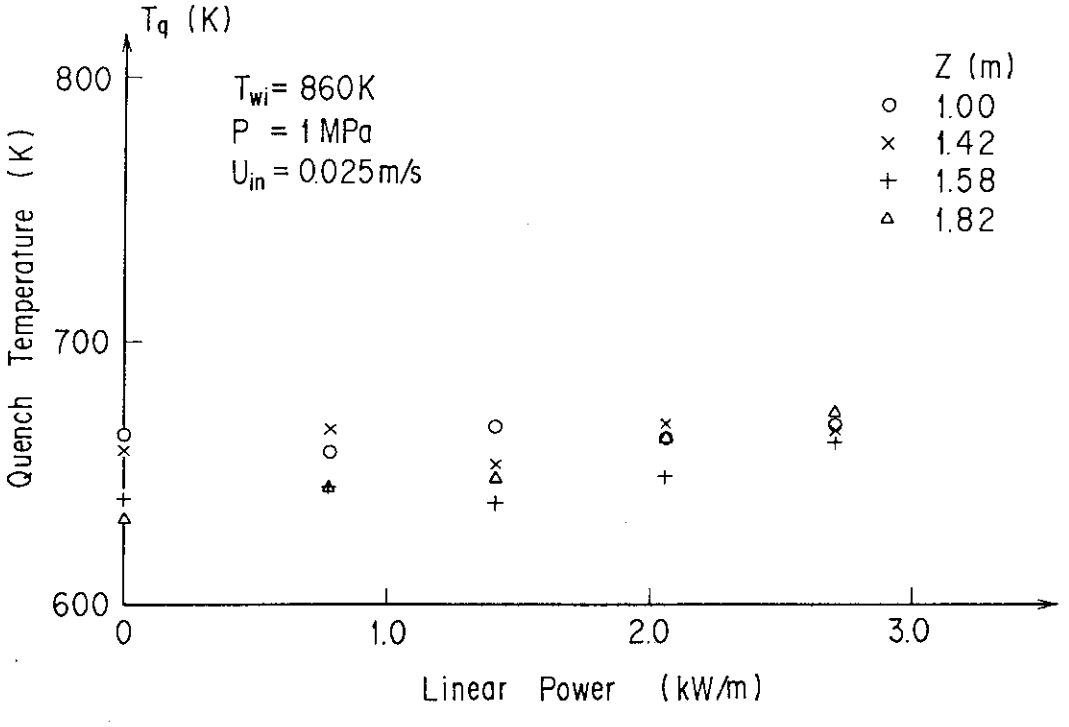

Fig. 18 Effect of linear power on quench temperature

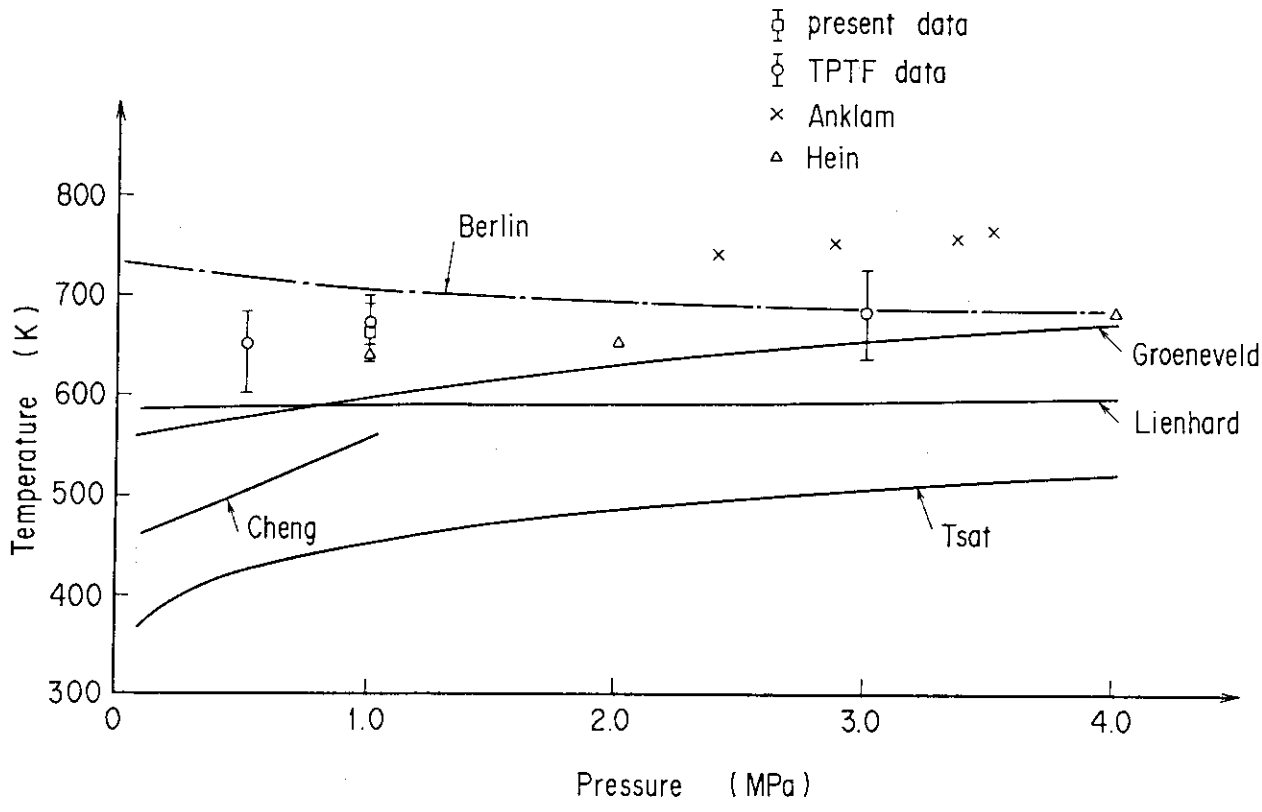

Fig. 19 Quench temperature

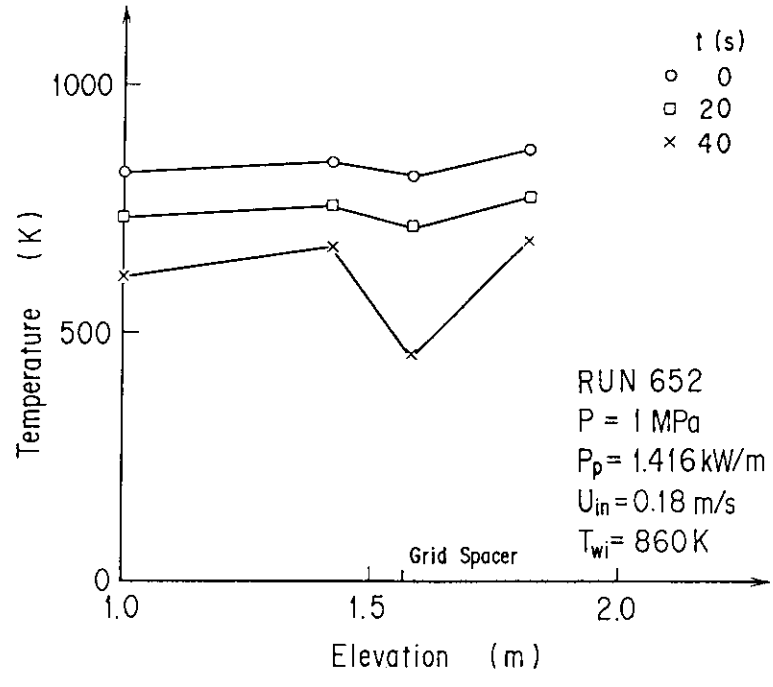

Fig. 20 Temperature profile along axial position

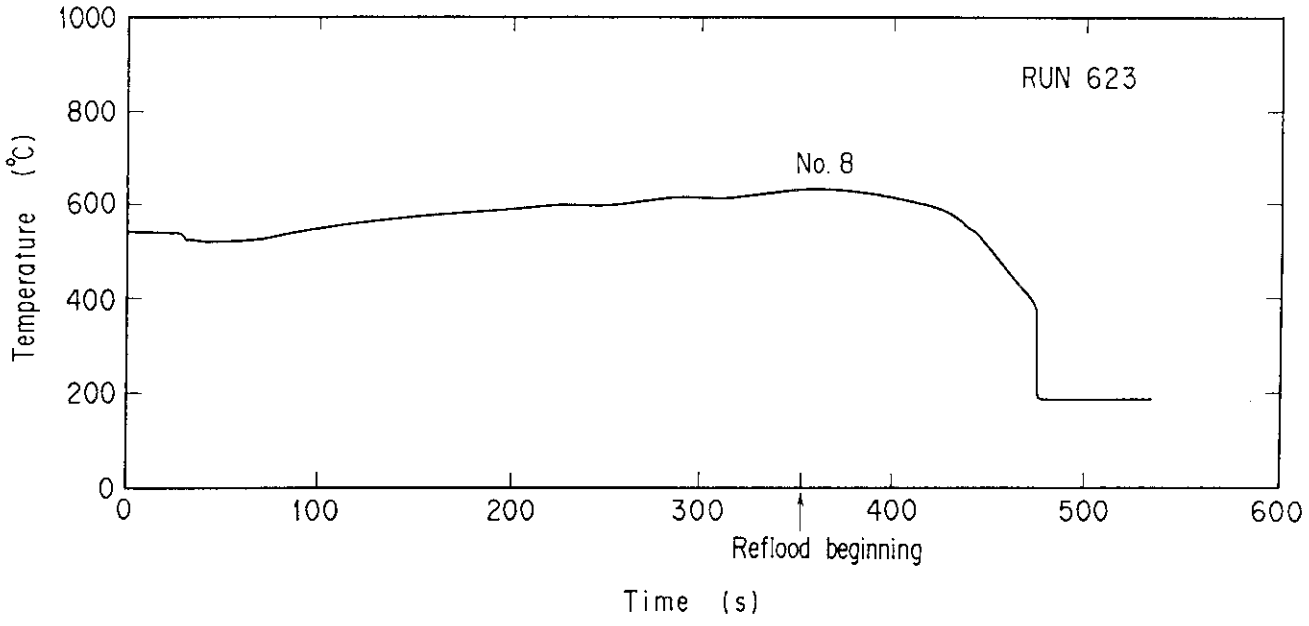

Fig. 21 Typical heater rod surface temperature transient

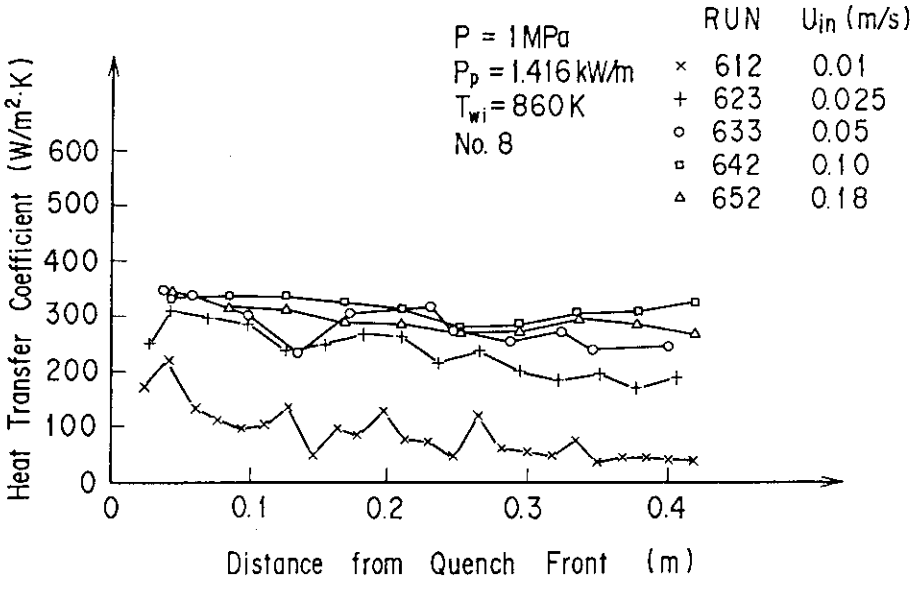

Fig. 22 Effect of reflooding flow rate on film boiling heat tarnsfer coefficient

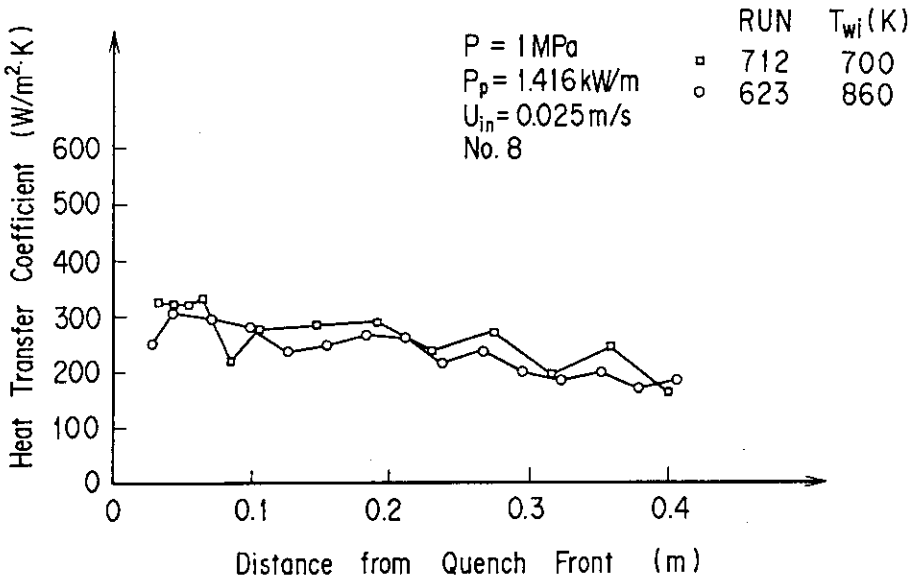

Fig. 23 Film boiling heat transfer coefficient under different initial surface tempeature

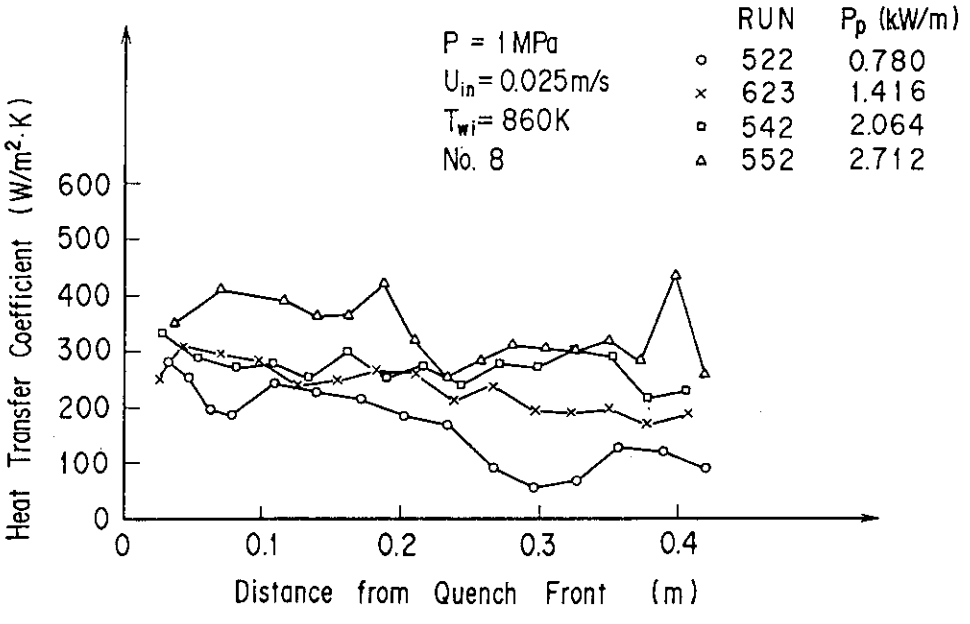

Fig. 24 Effect of linear power on film boiling heat transfer coefficient

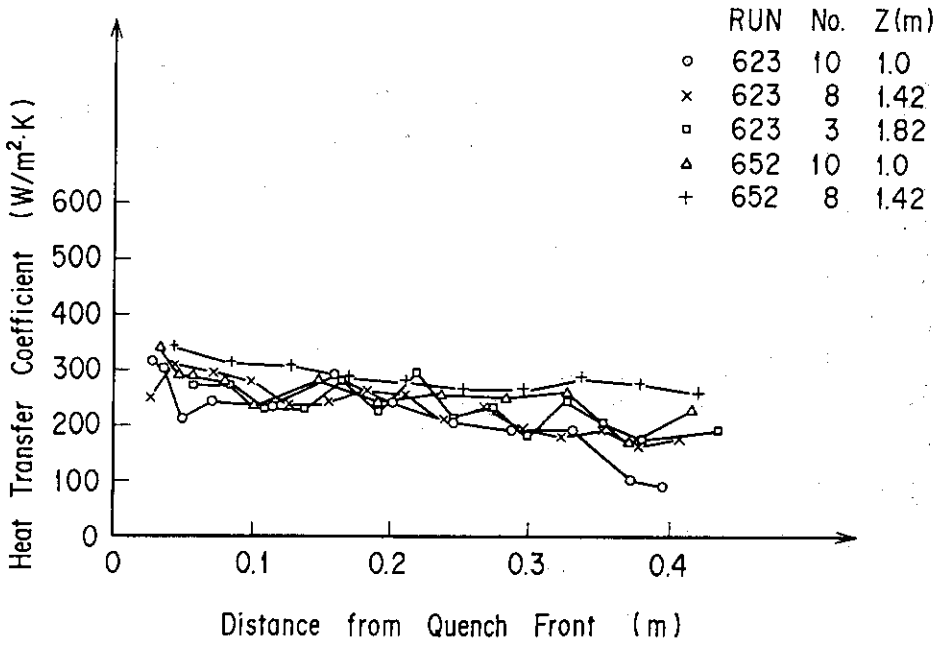

Fig. 25 Effect of elevation on film boiling heat transfer cofficient

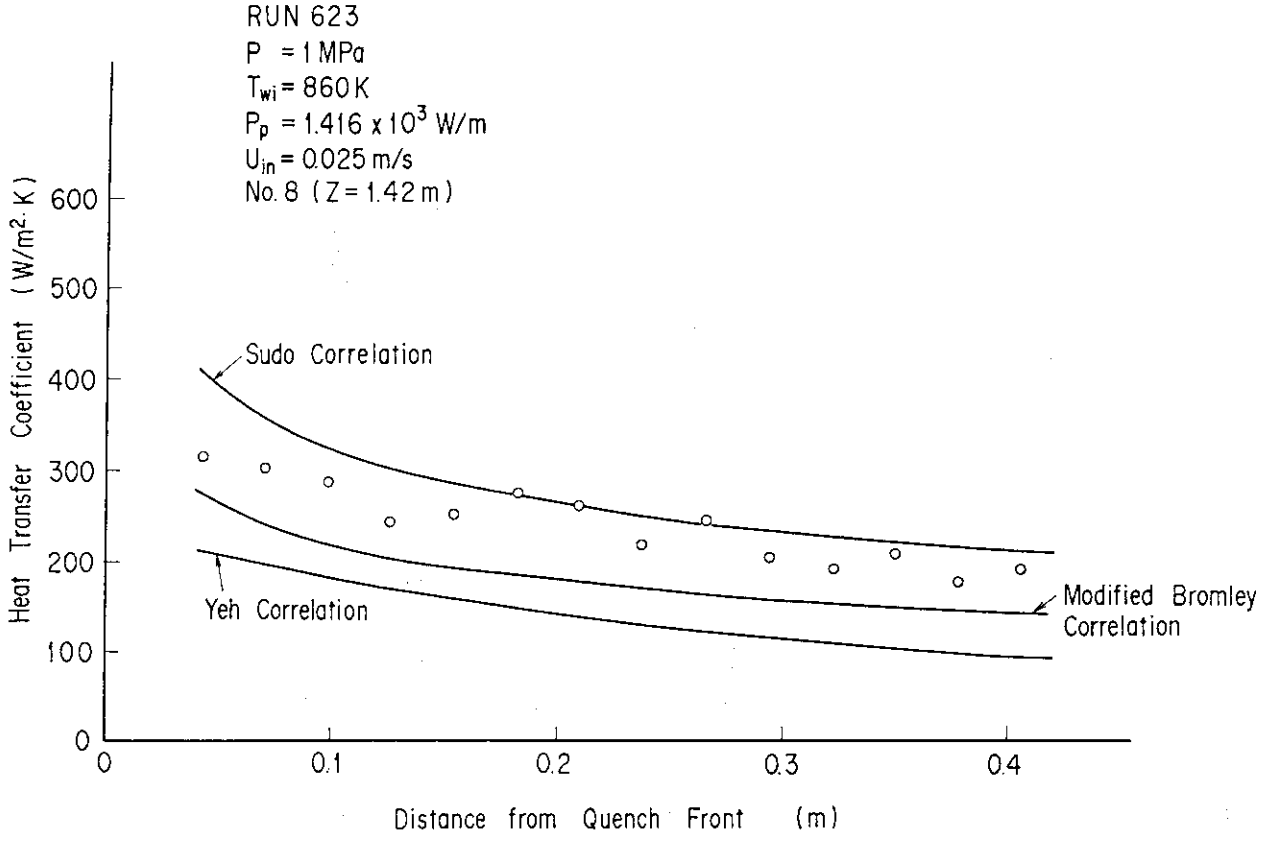

Fig. 26 Comparison of calculated and measured heat transfer coefficients

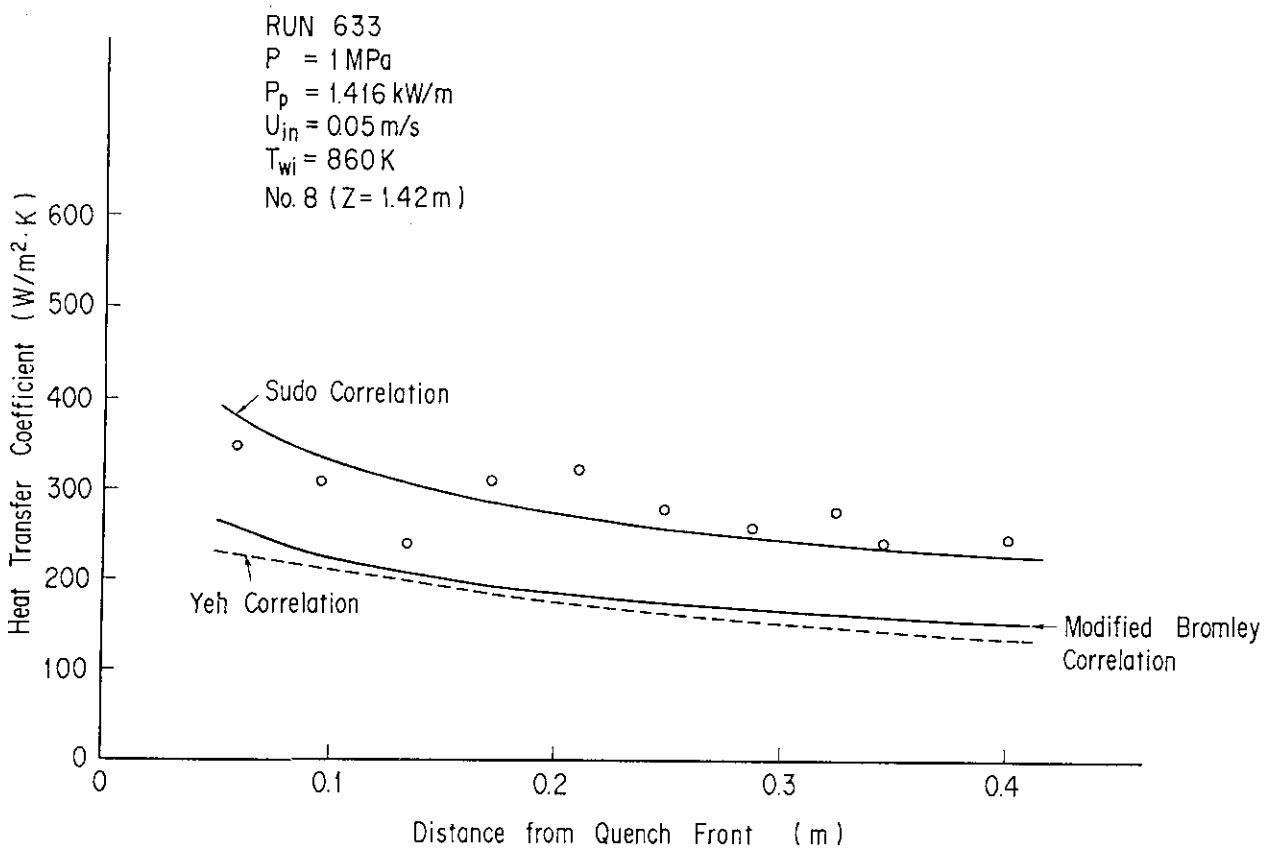

Fig. 27 Comparison of calculated and measured heat transfer coefficients

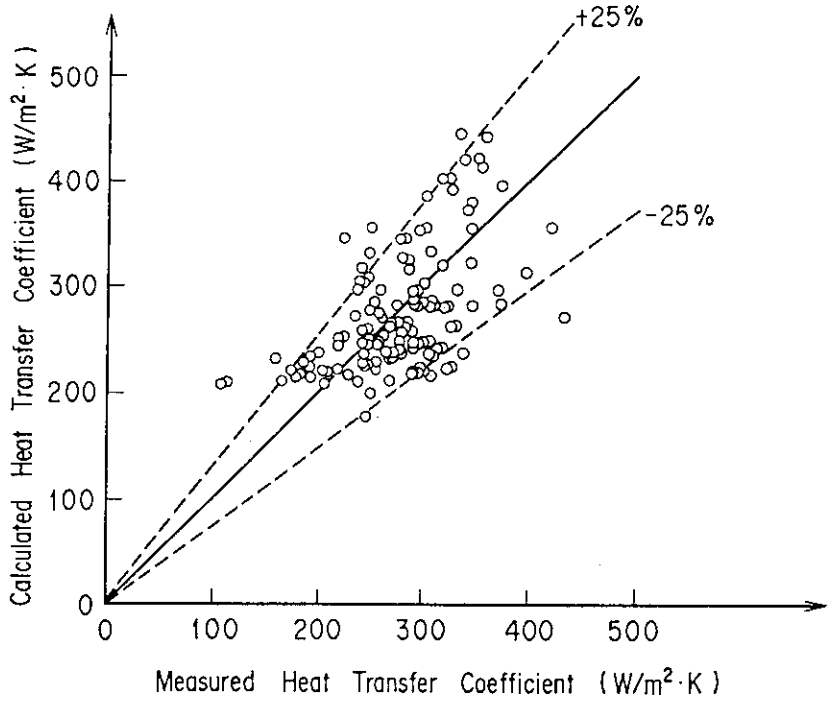

Fig. 28 Comparison of calculated and measured heat transfer coefficients